Faraday Discussion 'Single-Entity Electrochemistry'

High-bandwidth detection of short DNA in nanopipettes

Raquel Fraccari,[1] Marco Carminati,[2] Giacomo Piantanida,[2] Tina Leontidou,[1] Giorgio Ferrari,[2] Tim Albrecht[1]*

[1] Imperial College London, Department of Chemistry, Exhibition Road, London SW7 2AZ, UK

[2] Politecnico di Milano, Dipartimento di Elettronica, Informazione e Bioingegneria, P.za Leonardo da Vinci 32, Milano, Italy

Supporting Information

1) Gel characterization of the 100 and 200 bp DNA samples

Conditions: 2% agarose gel prestained with GelRed. Electric field: 5 V/cm

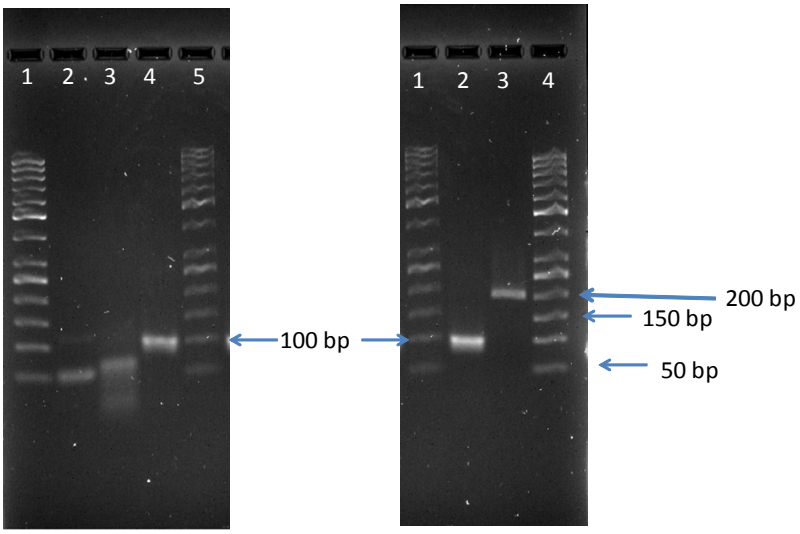

Fig. S1: Gel electrophoretic characterization of some of the DNA samples used in this study. Some DNA length indicated. Left: 50 bp DNA ladder (lane 1);100 nt ssDNA (lane 2); 100 nt ssDNA with 5' NH_2 modification (lane 3); 100 bp dsDNA (lane 4); 50 bp dsDNA ladder (lane 5). Right: 50 bp DNA ladder (lane 1); ds100 bp DNA (lane 2); ds200 bp DNA (lane 3); 50 bp DNA ladder (lane 4).

2) Additional noise characterization of the electronic setup

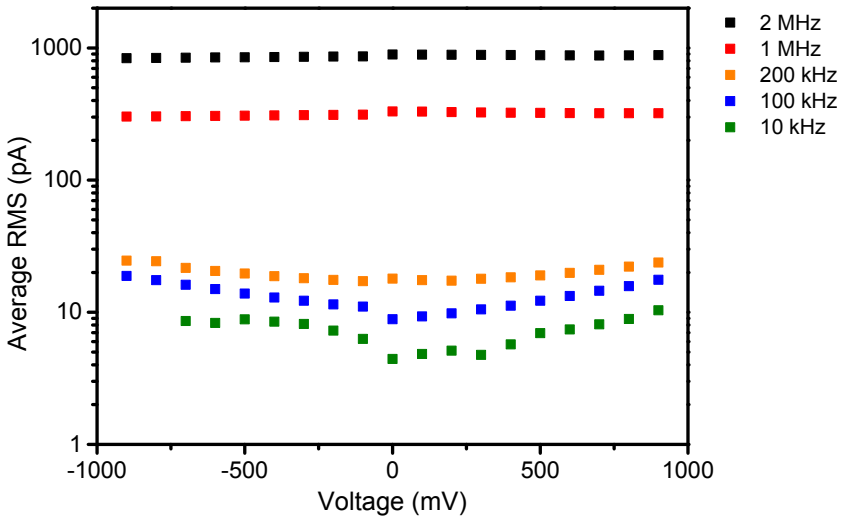

Fig. S2: Average RMS current noise in the AC channel as a function of V_{bias} at different filter frequencies for one of the pipettes used in this study. Solution conditions: 1 M KCl, 10 mM tris HCl, pH 8. At low frequencies, I_{rms}^{AC} increases with V_{bias}, which is due to Flicker noise (or another noise source that is proportional to the current). At high frequencies, I_{rms}^{AC} is dominated by the amplifier. Even at 2 MHz filter frequency, I_{rms}^{AC} is still below 1 nA.

3) Ion current/V_{bias} curves, examples

The pipette conductance is determined from the slope of an I/V_{bias} trace. While this is typically done at low V_{bias} (zero bias conductance), the I/V_{bias} curves are linear over a large V_{bias} range and show no rectification.

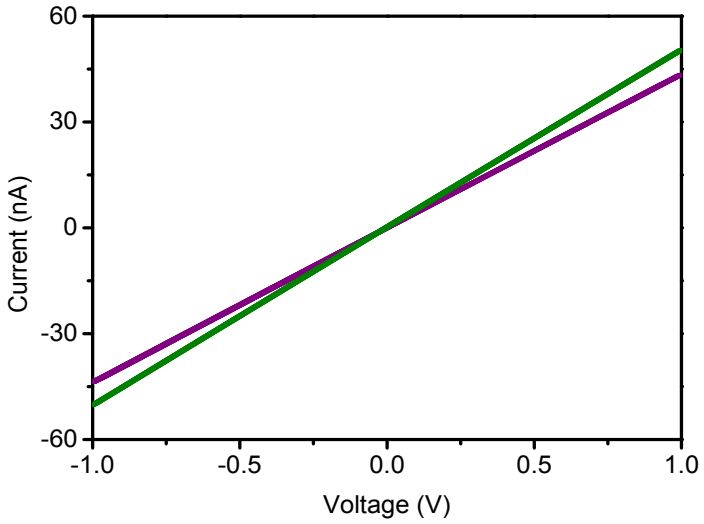

Fig. S3: Ion current/V_{bias} characteristics of two pipettes, pulled with the same programme 57 (see Methods section in main text). The conductance was determined to be 44 (purple) and 50 nS (green).

4) Estimate of the minimum detectable DNA length, $L_{DNA,m}$

We used data obtained for dsDNA in kilobasepair (kbp) range in 1 M KCl electrolyte to assess the capabilities of the current nanopipette platform (partly from Fraccari et al., Nanoscale 2016, 8, 7604-7611). The table below contains the translocation characteristics for each L_{DNA} and V_{bias}, as well as the instrumental settings. The average S/N ratio is 7.4 and appears to be roughly independent of the DNA sample (note that the filter frequencies change though).

V_{bias}	4 kbp	5.31 kbp	10 kbp	48.5 kbp
-200 mV	34 pA 0.170 ms 30 kHz 5.3 pA **6.4**	34 pA 0.304 ms 30 kHz 5.2 pA **6.6**	41 pA 0.524 ms 50 kHz 7.2 pA **5.7**	
-300 mV	59 pA 0.142 ms 60 kHz 8.4 pA **7.0**	58 pA 0.172 ms 60 kHz 8.1 pA **7.1**	55 pA 0.439 ms 50 kHz 8.0 pA **6.8**	53 pA 2.822 ms 20 kHz 5.4 pA **9.8**
-400 mV	76 pA 0.080 ms 100 kHz 12.1 pA **6.3**	82 pA 0.137 ms 100 kHz 13.3 pA **6.2**	84 pA 0.286 ms 100 kHz 12.7 pA **6.6**	74 pA 1.884 ms 30 kHz 9.1 pA **8.1**
-800 mV	191 pA 0.044 ms 200 kHz 25.3 pA **7.5**	188 pA 0.065 ms 200 kHz 25.6 pA **7.3**	215 pA 0.131 ms 200 kHz 29.3 pA **7.3**	229 pA 0.901 ms 100 kHz 19.9 pA **11.5**

Table S1: Translocation characteristics of long DNA from L_{DNA} = 4 - 48.5 kbp, as a function of V_{bias} (left column). Each cell contains I_{mp} [pA], τ_{mp} [ms], the filter frequency used [kHz], I_{rms}^{AC} [pA], and the S/N ratio I_{mp}/I_{rms}^{AC}.

Assuming that the S/N ratio does not change and that the scaling law for τ_{mp} remains valid for small L_{DNA}, we estimated the $L_{DNA,m}$ for which τ_{mp} = 10 µs from the scaling law ($\log(\tau_{mp}) \propto p \cdot \log(L_{DNA})$) for each V_{bias}. p values ranged from 1.17 to 1.24, but did not show any particular V_{bias}-dependence. The calculated $L_{DNA,m}$ values were 326 bp, 480 bp, 684 bp and 1152 bp for V_{bias} from -200 to -800 mV, as shown in table S1.

The following plot show $L_{DNA,m}$ vs. V_{bias}, where the dashed line is a linear fit (slope: -1.3569, intercept: 83.831). The latter allows extrapolating the estimate of $L_{DNA,m}$ to other, often used V_{bias}, e.g. V_{bias} = -50 mV (152 bp) and -100 mV (220 bp).

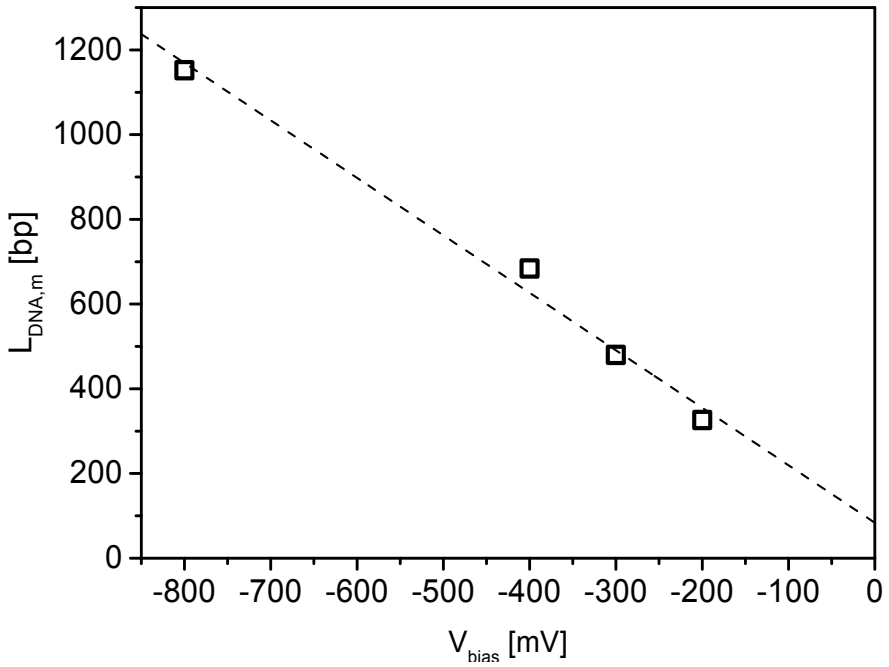

Fig. S4: Estimated $L_{DNA,m}$ vs. V_{bias} inc. linear fit (dashed line).

While this estimate provides a useful guideline to inform future experiments, its approximate nature has to be recognized. For example, while there is currently no study of the length dependence of τ_{mp} in this range of L_{DNA} with nanopipettes (to the best of the authors' knowledge), the extrapolation is rather long (from kbp to 100s of bp), *via* a double-logarithmic scaling representation, and is thus associated with a rather large error. Moreover, in doing so the DNA makes a transition from a long polymer L_{DNA} >> persistence length to a short one, L_{DNA} ≈ persistence length, so a change in the scaling law is likely. Nevertheless, as we show in the main text, the considerations above do have

some predictive power, in that $L_{DNA,m}$ indeed constitutes a limit of detection, at least under the experimental conditions here.

5) Additional information extracted from the translocation data

While τ and I_{mp} are both dependent on V_{bias}, it has been shown previously that the integral of the $I(t)$ trace during an event is specific to the analyte under study (the so-called 'event charge deficit', *ecd*, D. Fologea, E. Brandin, J. Uplinger, D. Branton, J. Li, Electrophoresis. 2007, 28, 3186-3192). In other words, for a given DNA sample, shorter events typically show larger I_{mp}, whereas slower events display lower I_{mp} values. Thus, for a given set of translocation data, e.g. for the same DNA at different V_{bias}, the *ecd* should be the same. That this is indeed the case for the data shown in the main manuscript is re-assuring, since it shows that the results are contaminated with impurities, external noise, or affected by instrumental settings/limitations.

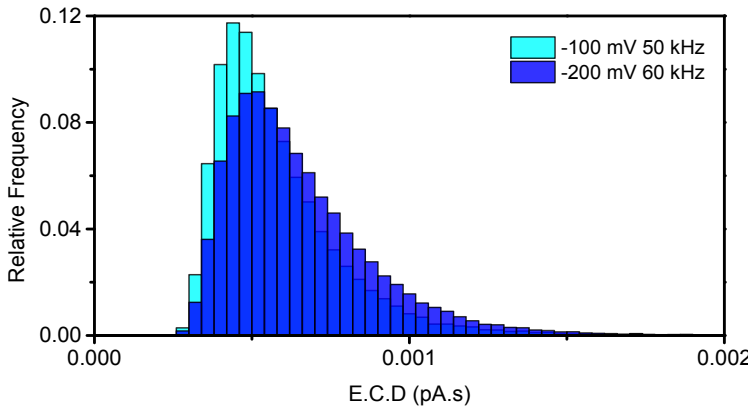

Fig. S5: *ecd* for the ranslocation of 200 bp dsDNA in 1 M KCl, as shown in Fig. 2 of the main manuscript. The two distributions strongly overlap, as expected.

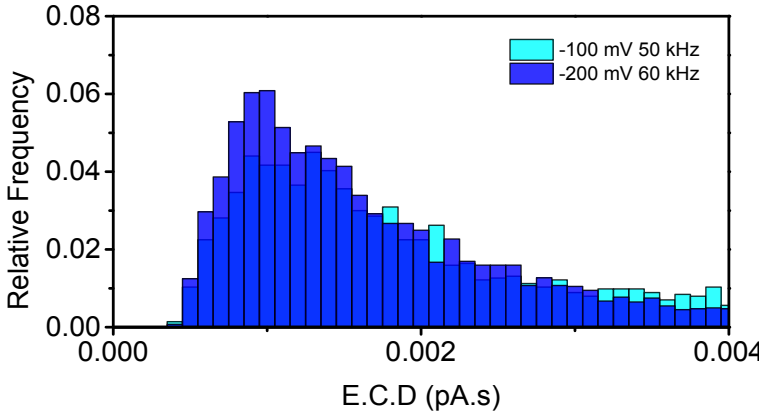

Fig. S6: *ecd* for the translocation of 100 bp dsDNA in 2 M LiCl, as shown in Fig. 3 of the main manuscript.

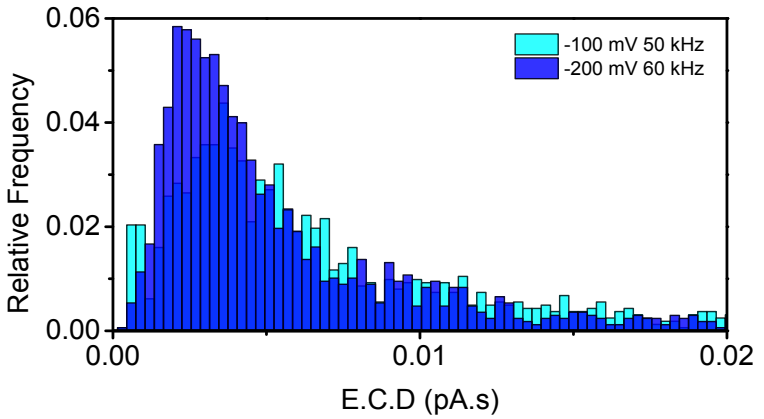

Fig. S7: *ecd* for the translocation of 100 bp dsDNA in 4 M LiCl, as shown in Fig. 4 of the main manuscript.

6) The effect of silanization of the quartz surface on the translocation of 'long' dsDNA

The translocation process can be strongly affected by surface modification, such as silanization. The proof-of-concept data shown below are a comparison of an unmodified and a modified pipette, with regards to the translocation of 10 kbp dsDNA (1 M KCl, V_{bias} = -500 mV). The modified pipette features a new cluster of events at longer τ_{mp} and higher I_{mp}, respectively. Whether the same holds for short dsDNA is currently unknown.

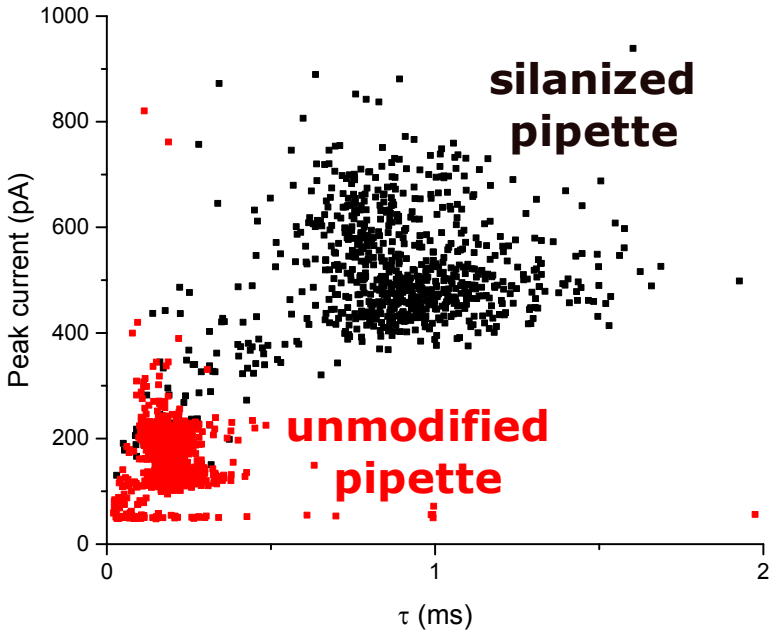

Fig. S8: Translocation of 10 kbp dsDNA in 1 M KCl, V_{bias} = -500 mV.